Turkish Journal of Earth Sciences (Turkish J. Earth Sci.), Vol. 19, 2010, pp. 409–429. Copyright ©TÜBİTAK
doi:10.3906/yer-0910-39 First published online 11 March 2010

Thermal Evolution of the Permo–Triassic Karakaya Subduction-accretion Complex between the Biga Peninsula and the Tokat Massif (Anatolia)

ILARIA FEDERICI[1], WILLIAM CAVAZZA[1], ARAL I. OKAY[2], OLIVIER BEYSSAC[3], MASSIMILIANO ZATTIN[4], SVEVA CORRADO[5] & FRANCESCO DELLISANTI[1]

[1] Department of Earth and Geoenvironmental Sciences, University of Bologna, 40127 Bologna, Italy
(E-mail: william.cavazza@unibo.it)

[2] Eurasia Institute of Earth Sciences, İstanbul Technical University, TR–34469 İstanbul, Turkey

[3] IMPMC, UMR 7590 CNRS-Paris 6-Paris 7-IPGP, 75252 Paris Cedex 05, France

[4] Department of Geosciences, University of Padua, via 8 Febbraio, 35122 Padua, Italy

[5] Department of Geological Sciences, University Rome3, Largo San Leonardo Murialdol, 00146 Rome, Italy

Received 27 October 2009; revised typescript received 01 February 2010; accepted 11 March 2010

Abstract: The results of the combined application of a series of analytical methods (clay mineralogy, vitrinite reflectance, Raman microspectroscopy) placed tight constraints on the thermal evolution of the Karakaya Complex of northern Anatolia, a mostly Permo–Triassic subduction-accretion complex resulting from the progressive closure of the Palaeotethys. The thermal evolution of the Karakaya Complex is the result of Permian–Triassic subduction-accretion processes, and was not significantly affected by later Alpine-age tectonism, as shown by Liassic shallow-water siliciclastic and carbonate deposits overlying unconformably the Karakaya Complex which did not undergo any significant burial. The Lower Karakaya Complex, comprising metabasite and subordinate marble and phyllite, experienced maximum temperatures ranging from 340 to 497° C, in agreement with independently determined thermobarometric reconstructions. The entire Upper Karakaya Complex, previously considered unmetamorphosed or slightly metamorphosed, was affected by zeolite to lower greenschist facies metamorphism (120–376° C). The coherent results of this study show that Raman thermometry has great potential for palaeotemperature determination at low temperature ranges (200–350° C).

Key Words: vitrinite reflectance, clay mineralogy, Raman thermometry, Karakaya Complex, Pontides

Biga Yarımadası ile Tokat Masifi Arasında Permo–Triyas Yaşlı Karakaya Dalma-batma-eklenme Kompleksinin Termal Evrimi

Özet: Bu çalışmada değişik analitik yöntemler (kil mineralojisi, vitrinit yansıması, karbonca zengin malzemenin Raman spektrometresi) kullanılarak Paleo-Tetis'in kapanması sürecinde oluşan, Permo–Triyas yaşındaki bir dalma-batma-eklenme birimini temsil eden Karakaya Kompleksi'nin termal evrimi araştırılmıştır. Karakaya Kompleksi üzerinde uyumsuzlukla yer alan, kuvvetli deformasyon veya gömülme yaşamamış Liyas yaşlı sığ denizel silisiklastik ve karbonat kayaları, Karakaya Kompleksi'nin termal evriminin büyük ölçüde Permo–Triyas yaşlı dalma-batma süreçlerine bağlı olduğunu ve daha sonraki Alpin olaylardan fazla etkilenmediğini göstermektedir. Metabazitlerden ve daha az oranlarda mermer ve fillattan oluşan Alt Karakaya Kompleksi 340 ile 497°C arasında değişen maksimum sıcaklıklara ulaşmıştır. Daha önceki çalışmalarda metamorfik olmadığı veya çok düşük dereceli metamorfizma geçirdiği farz edilen, Üst Karakaya Kompleksi ise zeolit ve yeşilşist fasiyesinde (120–376°C) metamorfizma geçirmiştir. Bu çalışmanın sonuçları Raman termometresinin nispeten düşük sıcaklıkları (200–350°C) tanımlamakta büyük potansiyel taşıdığını göstermektedir.

Anahtar Sözcükler: kil mineralojisi, vitrinit yansıması, Raman termometresi, Karakaya Kompleksi, Pontidler

Introduction

The Karakaya Complex is the tectonostratigraphic term used to designate the strongly deformed Permo–Triassic rock units in the Sakarya terrane (Sakarya Composite Terrane of Göncüoğlu et al. 2000; also known as Sakarya Zone) of northern Anatolia (Figure 1). This complex developed during Permo–Triassic northward subduction of the Palaeotethys Ocean along the southern margin of Eurasia (Tekeli 1981; Pickett & Robertson 1996; Okay 2000; Stampfli & Borel 2004).

Although the pre-Jurassic rocks of the Sakarya terrane had been described and mapped by several authors in previous years, the comprehensive term Karakaya Formation was first defined by Bingöl *et al.* (1975), who supported an intracontinental rift origin for this unit. Conversely, Tekeli (1981) proposed a subduction-accretion origin. The Karakaya Formation was renamed Karakaya Complex by Şengör *et al.* (1984). Several other studies have dealt with the Karakaya Complex (e.g., Akyürek & Soysal 1983; Akyürek *et al.* 1984; Koçyiğit 1987; Kaya et al. 1986; Okay *et al.* 1991; Altıner & Koçyiğit 1993; Pickett & Robertson 1996; Yılmaz *et al.* 1997; Göncüoğlu *et al.* 2000, 2004; Okay & Altıner 2004; Yılmaz & Yılmaz 2004) yet the same two geodynamic interpretations are still in competition: the rift model and the subduction-accretion one, each with several different variations (Yılmaz 1981; Şengör & Yılmaz 1981; Şengör 1984; Şengör *et al.* 1984; Koçyiğit 1987; Genç & Yılmaz 1995; Göncüoğlu *et al.* 2000; Pickett & Robertson 1996, 2004; Okay 2000).

There is general agreement that the Karakaya Complex is restricted to the Sakarya terrane of the Pontides and is absent in the rest of the Pontides and in the Anatolide-Tauride Block (Okay & Göncüoğlu 2004) (Figures 1 & 3). Two tectonostratigraphic units were defined in the Karakaya Complex: the first one consisting of metabasite, phyllite and marble, the second one comprising highly deformed epiclastic and volcaniclastic rocks generally considered unmetamorphosed or slightly metamorphosed (e.g. Pickett 1994). Following Okay & Göncüoğlu (2004), the terms Lower and Upper Karakaya Complex are used here for the metabasite series and the clastic series, respectively.

In this contribution we determine in the Lower and Upper Karakaya Complex (i) clay mineral metamorphism using XRD diffraction-derived parameters such as the Kübler Index and the percentage of illite in I-S mixed layers, and (ii) organic metamorphism by means of vitrinite reflectance data and Raman spectroscopy on carbonaceous material (RSCM). These temperature-dependent parameters have been successfully applied in better known regions where very low- to low-grade metamorphic rocks are exposed to constrain the thermal structures of high crustal levels (e.g., Beyssac *et al.* 2004, 2007; Potel *et al.* 2006; Judik *et al.* 2008). Clay mineral parameters such as the Kübler Index and the percentage of illite in I-S mixed layers, coupled with vitrinite reflectance are traditionally used to constrain thermal conditions from diagenesis to epizone (Ferreiro Mählmann 2001; Rantitsch *et al.* 2005; Potel *et al.* 2006), and their correlations have been widely explored both in diagenetic (Corrado *et al.* 2005; Aldega *et al.* 2007a, b) and metamorphic conditions (Potel *et al.* 2006). Raman spectroscopy has been applied widely to provide reliable estimates of peak metamorphic temperatures between 350° and 650° C (Beyssac *et al.* 2002, 2003, 2004, 2007; Rantitsch *et al.* 2004; Negro et al. 2006): a recent pilot study focused on temperature below 350° C (Lahfid 2008).

Geological Setting

The study area is located in the Sakarya terrane, an east–west-trending continental block about 1,500 km long and 120 km wide (Figure 1). To the northwest the Sakarya terrane is in tectonic contact with the İstanbul terrane along the Intra-Pontide suture, and to the north it is bounded by the Black Sea. The contact with the Anatolide-Tauride Block to the south is marked by the İzmir-Ankara-Erzincan suture. Outcrops of the Permo–Triassic, highly deformed, low-grade metamorphic rocks of the Karakaya Complex characterize the Sakarya terrane over a distance of ca. 1,100 km from the Biga Peninsula to the Lesser Caucasus. The Sakarya terrane, together with the İstanbul and Strandja terranes, shows Laurasia affinities (Okay & Tüysüz 1999) with Palaeozoic and Mesozoic stratigraphies different from the Anatolide-Tauride Block to the south. These terranes were amalgamated into a

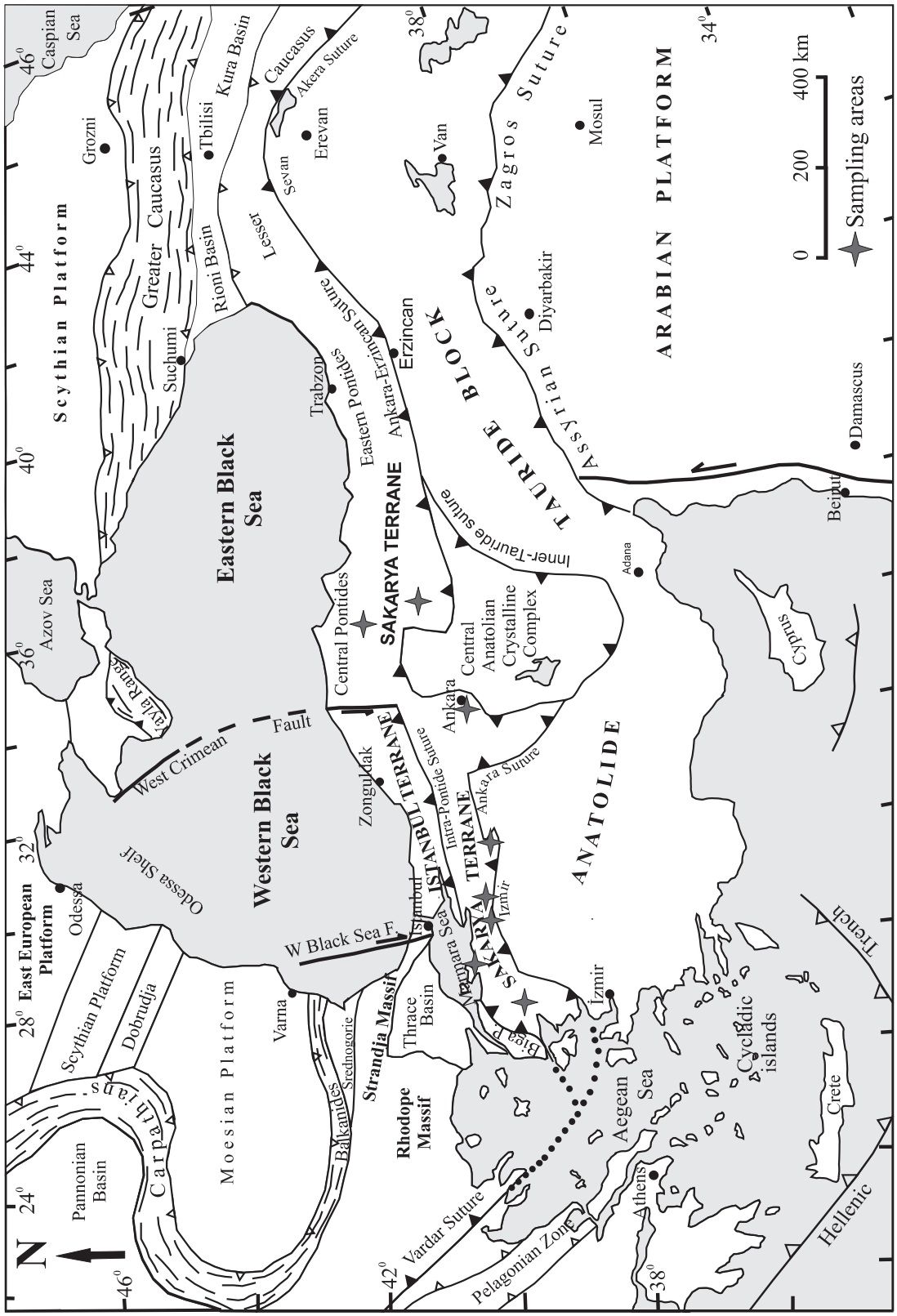

Figure 1. Simplified tectonic map of Turkey and the surrounding regions. Modified from Okay & Tüysüz (1999).

single continental unit during the latest Cretaceous–Palaeocene continental collision (Şengör & Yılmaz 1981; Okay & Tüysüz 1999).

The Karakaya Complex is subdivided into a low-grade metamorphic series [Lower Karakaya Complex (LKC), also known as Nilüfer Unit] and a clastic series [Upper Karakaya Complex (UKC)] comprising three tectonostratigraphic units consisting of highly deformed epiclastic and volcaniclastic rocks (Hodul, Orhanlar and Çal units) (Figure 2). The UKC is traditionally considered unmetamorphosed or slightly metamorphosed.

The LKC consists of highly deformed and metamorphosed metabasite, phyllite and marble, with minor amounts of metachert, metagabbro and serpentinite (Okay & Göncüoğlu 2004). Rocks of the LKC are generally foliated, isoclinally folded and cut by a large number of shear zones. The original thickness is difficult to estimate but the structural thickness exceeds 5 km (Okay & Göncüoğlu 2004). Conodonts from marble interbedded with the metabasite gave an Early Triassic age from the type locality of the LKC south of Bursa and a Middle Triassic age from the Biga peninsula (Kaya & Mostler 1992; Kozur *et al.* 2000).

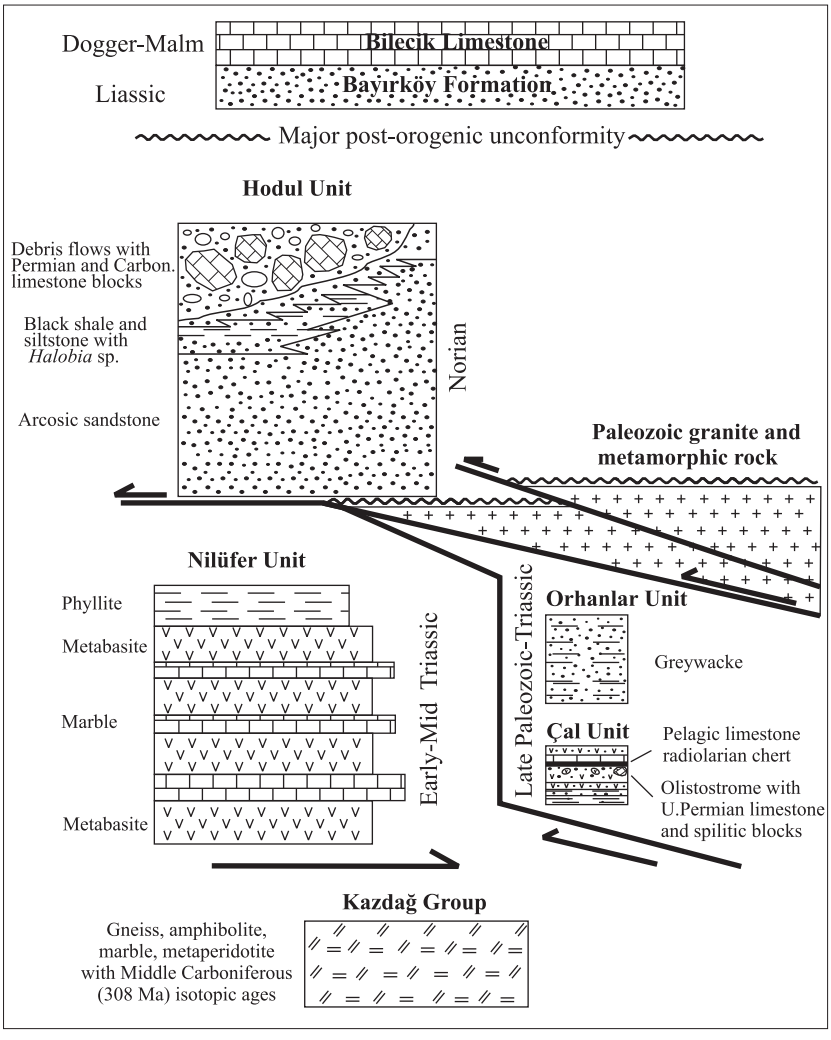

Figure 2. Tectono-stratigraphy of the Karakarya Complex showing the tectonic relationships between its Lower and Upper portions. Modified from Okay (2000).

The LKC is metamorphosed under greenschist facies conditions, with a common mineral paragenesis of actinolite/barroisite + albite + chlorite + epidote in the metabasite (Okay & Monié 1997; Okay 2000; Okay *et al.* 2002). Locally, metamorphism reaches albite-epidote amphibolite, blueschist, and eclogite facies (Okay & Monié 1997; Okay et al. 2002; Okay & Göncüoğlu 2004). The blueschist and eclogite facies rocks form tectonic slices within the predominantly greenschist facies rocks. Ar-Ar isotopic ages from phengite and amphibole from an eclogite lens enclosed into the greenschist facies east of Bandırma (Okay & Monié 1997) and from blueschist and high-pressure greenschist facies metabasite north of Eskişehir (Okay *et al.* 2002) yielded very similar Late Triassic (205–203 Ma) ages. The LKC of the eastern Pontides yielded early Permian (263–260 Ma) Ar-Ar and Rb-Sr ages (Topuz *et al.* 2004a, b).

The relationship between the LKC and the epiclastic and volcaniclastic rocks of the UKC are almost everywhere tectonic. The UKC consists of three tectonostratigraphic units made of highly deformed epiclastic and volcaniclastic rocks (Figure 2). The highly deformed nature of these units makes their identification and correlation across the Sakarya terrane problematic (Okay & Göncüoğlu 2004). However, there is a general agreement, at least in the western outcrop area, that the UKC includes a thick quartzo-feldspathic sandstone-shale series (Hodul Unit) with a continental granitic source, and a greywacke-shale sequence (Orhanlar Unit). The UKC also comprises a series of basalt, debris flows, and grain flows containing Upper Permian limestone clasts (Çal Unit) (Okay *et al.* 1991; Pickett & Robertson 1996; Okay & Göncüoğlu 2004). In this paper, we extend tentatively this stratigraphic subdivision to our entire study area. Outside of their type localities in the area of the Biga peninsula, the terms Hodul Unit and Orhanlar Unit as used in this study refer generically to arkosic sandstones and graywackes, respectively, belonging to the upper structural levels of the Karakaya Complex (for a description, see below). Currently, a rigorous tectonostratigraphic correlation throughout the entire outcrop area of the Karakaya Complex is hampered by the high degree of structural complexity combined with the scarcity of detailed regional studies.

The *Hodul Unit* crops out from the Biga Peninsula in the west to the region north of Eskişehir, and consists of arkosic sandstones with intercalation of shales and siltstones, which pass upward into olistostromes and debris flows with blocks of basalt and Carboniferous and Permian limestone (Okay *et al.* 1991; Leven & Okay 1996). Arkosic sandstone ranges from coarse-grained, thickly bedded proximal facies with pebbles of granite to finer-grained distal turbidites. The arkosic sandstone succession is attributed to the Norian, mainly based on a few occurrences of *Halobia* sp. (Kaya *et al.* 1986; Wiedmann *et al.* 1992; Leven & Okay 1996; Okay & Altıner 2004). The presence of Ladinian limestone blocks in the Bursa area (Wiedmann *et al.* 1992) may indicate a longer time span for the Hodul Unit.

The Hodul Unit is strongly deformed with anastomosing shear zones and boudinage obscuring original bedding at all scales, from outcrop to thin section. The estimated total thickness of this unit is >2 km (Okay 2000): a more precise determination is hampered by strong deformation. The Hodul Unit is unconformably overlain by fairly undeformed shallow-water Liassic sandstone and siltstone (Bayırköy Formation, Figure 2).

The bulk of the *Orhanlar Unit* (>80%) consists of yellowish green, yellowish brown, highly fractured and generally altered greywacke that rarely shows recognizable bedding (Okay *et al.* 1991). These rocks are composed of very poorly sorted angular quartz, plagioclase, opaque minerals, black metachert, red radiolarian chert, basalt and phyllite clasts set in an argillaceous matrix. In the type locality near Orhanlar village, the greywacke series contains small (<1 m) olistoliths of dark Lower Carboniferous (Visean and Serpukhovian) limestone and is overlain by undeformed Liassic sandstones and siltstones (Leven & Okay 1996). The Orhanlar Unit shows strong layer-parallel extension that has destroyed much of the original bedding. However, its thickness probably ranges from a few hundred metres to over 1 km. Okay *et al.* (1991) described the origin of the Orhanlar Unit as related to an accretionary complex dominated by trench fan and axial channel deposits.

The *Çal Unit* (Figure 2) consists mainly of grain and debris flows and olistostromes with basalt and Upper Permian limestone clasts. The siliciclastic mass flows are interbedded with basaltic lava flows, calciturbidites, pelagic limestone, shale, greywacke and rare radiolarian chert (Okay et al. 1991; Okay & Göncüoğlu 2004). A typical feature of this unit is the presence of fossiliferous Upper Permian limestone blocks and olistoliths ranging in size from a few centimetres to one kilometre. The debris-flow deposits are distinguished from those of the Hodul Unit by the abundance of spilitized basic volcanic rocks (Sayıt & Göncüoğlu 2009). The Çal Unit is also strongly deformed, and hence the stratigraphic relationships of this unit, if any, with the other units of the UKC are obscure.

The tectonic evolution of the Karakaya Complex is still matter of debate. In the rift model proposed by Bingöl *et al.* (1975) and then developed by Şengör & Yılmaz (1981), Şengör *et al.* (1984), Şengör (1984), Genç & Yılmaz (1995), and Göncüoğlu (2000), the Karakaya Complex was deposited in a late Permian rift, which developed in a small marginal basin and closed in the late Triassic by southward subduction. Initially Bingöl *et al.* (1975) assumed that the Karakaya rift was purely intracontinental, but the presence of oceanic crustal lithologies in the Karakaya Complex led to the suggestion that the Karakaya rift developed into an oceanic marginal basin (Şengör & Yılmaz 1981). In this model, it is assumed that the Karakaya marginal basin opened on the northern margin of the Anatolide-Tauride Block above the southward subducting Palaeotethys Ocean and that the Permian and Carboniferous limestone blocks are derived from uplifted rift shoulders.

The subduction-accretion model was first proposed by Tekeli (1981) and then developed by Pickett & Robertson (1996), and Okay (2000). This model assumes that the Karakaya Complex was formed during the late Permian–Triassic by northward subduction-accretion of the Palaeotethys under the active Laurasian margin. The units of the Karakaya Complex were formed either during the steady-state subduction of oceanic crust, or, during subduction of oceanic seamounts (Pickett & Robertson 2004) or an oceanic plateau (Okay 2000).

Sampling

Samples were collected from suitable rock types over a distance of about 800 km from the Biga peninsula to the Tokat Massif (Figures 1 & 3). Samples from the Biga peninsula, Bandırma and Bursa are from the type areas of the Karakaya Complex. The remaining samples come from the Ankara area, the Tokat Massif and the Kargı Massif, where the lithological assemblage has been correlated with the Karakaya Complex of Biga, Bandırma, and Bursa (Yılmaz & Yılmaz 2004; Okay 2000; Okay & Göncüoğlu 2004; Pickett & Robertson 2004).

Twenty samples were collected for clay mineralogy analysis, mainly from clay and silt layers of the Hodul and Orhanlar units of the UKC. Only two samples were taken from the phyllite of the LKC. Twelve samples were collected for vitrinite reflectance analysis from the same localities, mainly from the arenaceous and pelitic beds of the Hodul and Orhanlar units. Seventeen samples were collected in the same localities for Raman spectroscopy (RSCM) from both the Upper (Hodul and Orhanlar units) and Lower Karakaya Complex. The results of these analyses are reported in Tables 1 and 2.

Methods

Clay Mineralogy

The bulk rock mineralogical composition of the clay fraction was determined by powder X-ray diffraction (XRD) using a Philips PW 1710 diffractometer (CuKα radiation; 40kV/30 mA power supply; graphite secondary monochromator, 1° divergence and scatter slits, 0.1 mm receiving slit; 0.02° 2θ step size; counting time of 2 s/step).

Clay mineralogy was determined on the <2μm grain-size fraction by XRD. Following the recommendations by Kisch (1991), the <2μm fraction was obtained by differential settling after disintegration by shaking in demineralized water and ultrasonic disaggregation for up to 15 minutes. Both air-dried and ethylene glycol solvated samples (50° C overnight) were analyzed by XRD. Smeared oriented mounts were prepared for each sample taking into account that the amount of clay on the glass slide was at least 3mg/cm^2 (Lezzerini *et al.*

Table 1. Clay mineralogy and vitrinite reflectance data and Raman spectroscopy temperatures.

Locality		Sample	Coordinates	Unit	Lithology	%Ro±s.d. (n. measurements)	KI (001) 10Å	ÁI (002) 7Å	% I in I/S (<2μm)	X-Ray semiquantitative analyses		RSCM (T°C)
										bulk	<2μm	
Biga Peninsula	Havran	IF 24	N39°35'53.018" E27°10'49.364"	Hodul Unit	dark brown siltite with numerous mineral fragments and macrofossils, alterated	1.377±0.14 (45)	0.95		80	$Ms_{25}Chl_{15}Qtz_{40}Pl_{20}$	$Ill_{45}Chl_{45}I/S_{1}$	
		IF 23	N39°36'05.265" E27°10'58.537"	Hodul Unit	medium-grained greenish brown sandstone, alterated	0.97±0.07 (21)						
	Balya	IF 17	N39°44'27.208" E27°35'29.662"	Hodul Unit	fine-grained greenish brown sandstone	0.74±0.09 (42)						
		IF 19	N39°44'48.299" E27°35'53.373"	Hodul Unit	dark grey argillite	1.984±0.06 (55)	0.86		90	$Ms_{25}Chl_{15}Qtz_{30}Pl_{30}$	$Ill_{74}Chl_{25}I/S_{1}$	
		IF 20	N39°44'16.031" E27°39'39.086"	Hodul Unit	fine-grained greenish brown siltite	0.934±0.09 (33)						
	Orhanlar	IF 13	N39°53'04.123" E27°36'53.926"	Orhanlar Unit	fine- to medium-grained grey greywacke with vein of calcite	1.039±0.04 (15)						
Bandırma		IF 28	N40°21'14.582" E28°00'20.098"	Hodul Unit	brown grey mudstone with slaty cleavage		0.26			$Ms_{63}Chl_{10}Qtz_{5}K\text{-}fd_{10}Pl_{10}$	$Ill_{95}C/S_{5}$	270±30
		IF 29	N40°21'14.582" E28°00'20.098"	Hodul Unit	brown grey mudstone with slaty cleavage		0.25			$Ms_{65}Chl_{10}Qtz_{5}K\text{-}fd_{5}Pl_{10}Cal_{5}$	$Ill_{85}Chl_{10}C/S_{5}$	270±30
		IF 31	N40°21'14.099" E28°00'19.794"	Hodul Unit	brown grey mudstone with slaty cleavage		0.22			$Ms_{60}Chl_{5}Qtz_{15}K\text{-}fd_{5}Pl_{5}Cal_{10}$	$Ill_{95}C/S_{5}$	270±30
		IF 33	N40°21'14.582" E28°00'20.098"	Hodul Unit	brown grey mudstone with slaty cleavage and veins of calcite	3.306±0.10 (26)	0.19			$Ms_{5}Chl_{5}Qtz_{20}Pl_{5}Cal_{65}$	$Ill_{85}Chl_{10}C/S_{5}$	270±30
		IF 34	N40°21'14.841" E28°00'20.187"	Hodul Unit	brown grey mudstone with slaty cleavage and veins of calcite		0.22			$Ms_{15}Chl_{5}Qtz_{25}Pl_{15}Cal_{40}$	$Ill_{90}Chl_{5}C/S_{5}$	270±30
Bursa area	SW	7249	N40°04'43.240" E29°00'22.452"	Nilüfer Unit	phyllites							340±30
		7370	N40°05'50.376" E28°56'28.779"	Nilüfer Unit	marble							340±30
		7369	N40°10'34.850" E28°58'26.259"	Nilüfer Unit	marble							405±24
		IF 36	N40°04'25.935" E28°59'53.575"	Orhanlar Unit	dark grey mudstone with slaty cleavage	3.177±0.13 (36)	0.23	0.26		$Ms_{10}Chl_{20}Qtz_{15}Pl_{10}Cal_{5}$	$Ill_{60}Chl_{40}$	
		IF 37	N40°04'25.935" E28°59'53.575"	Orhanlar Unit	dark grey mudstone with slaty cleavage		0.26	0.26		$Ms_{30}Chl_{25}Qtz_{20}Pl_{25}$	$Ill_{50}Chl_{50}$	340±30
		IF 39	N40°04'23.375" E28°59'08.330"	Orhanlar Unit	grey mudstone	1.747±0.09 (46)	0.52	0.44	95	$Ms_{15}Chl_{15}Qtz_{35}Pl_{35}$	$Ill_{65}Chl_{35}$	
	NE	IF 7	N40°15'34.206" E29°13'01.968"	Hodul Unit	grey mudstone	1.176±0.08 (51)	0.92		85	$Ms_{25}Qtz_{55}Pl_{20}$	$Ill_{99}I/S_{1}$	

Note: %Ro -vitrinite reflectance; KI -Kübler Index; ÁI -Árkai Index; %I in I/S -illite content in illite-smectite; RSCM -raman spectroscopy on carbonaceous material; Ms -muscovite; Chl -chlorite; Qtz -quartz; K-feldspar; Pl -plagioclase; Cal -calcite; Kln -kaolinite Ill -illite; I/S -illite/smectite; C/S -chlorite/smectite.

Table 1. Continued.

Locality		Sample	Coordinates	Unit	Lithology	%Ro±s.d. (n. measurements)	KI (001) 10Å	ÁI (002) 7Å	% I in I/S (<2µm)	X-Ray semiquantitative analyses		RSCM (T°C)
										bulk	<2µm	
Biga Peninsula	Havran	IF 24	N39°35'53.018" E27°10'49.364"	Hodul Unit	dark brown siltite with numerous mineral fragments and macrofossils, alterated	1.377±0.14 (45)	0.95		80	$Ms_{25}Chl_{15}Qtz_{40}Pl_{20}$	$Ill_{45}Chl_{55}I/S_1$	
		IF 23	N39°36'05.265" E27°10'58.537"	Hodul Unit	medium-grained greenish brown sandstone, alterated	0.97±0.07 (21)						
	Balya	IF 17	N39°44'27.208" E27°35'29.662"	Hodul Unit	fine-grained greenish brown sandstone	0.74±0.09 (42)						
		IF 19	N39°44'48.299" E27°35'53.373"	Hodul Unit	dark grey argillite	1.984±0.06 (55)	0.86		90	$Ms_{25}Chl_{15}Qtz_{30}Pl_{30}$	$Ill_{74}Chl_{25}I/S_1$	
		IF 20	N39°44'16.031" E27°39'39.086"	Hodul Unit	fine-grained greenish brown siltite	0.934±0.09 (33)						
	Orhanlar	IF 13	N39°53'04.123" E27°36'53.926"	Orhanlar Unit	fine- to medium-grained grey greywacke with vein of calcite	1.039±0.04 (15)						
Bandırma		IF 28	N40°21'14.582" E28°00'20.098"	Hodul Unit	brown grey mudstone with slaty cleavage		0.26			$Ms_{65}Chl_{10}Qtz_5K\text{-}fd_{10}Pl_{10}$	$Ill_{95}C/S_5$	270±30
		IF 29	N40°21'14.582" E28°00'20.098"	Hodul Unit	brown grey mudstone with slaty cleavage		0.25			$Ms_{65}Chl_{10}Qtz_5K\text{-}fd_5Pl_{10}Cal_5$	$Ill_{85}Chl_{10}C/S_5$	270±30
		IF 31	N40°21'14.099" E28°00'19.794"	Hodul Unit	brown grey mudstone with slaty cleavage		0.22			$Ms_{60}Chl_5Qtz_{15}K\text{-}fd_5Pl_5Cal_{10}$	$Ill_{95}C/S_5$	270±30
		IF 33	N40°21'14.582" E28°00'20.098"	Hodul Unit	brown grey mudstone with slaty cleavage and veins of calcite	3.306±0.10 (26)	0.19			$Ms_5Chl_5Qtz_{20}Pl_5Cal_{65}$	$Ill_{85}Chl_{10}C/S_5$	270±30
		IF 34	N40°21'14.841" E28°00'20.187"	Hodul Unit	brown grey mudstone with slaty cleavage and veins of calcite		0.22			$Ms_{15}Chl_5Qtz_{25}Pl_{15}Cal_{40}$	$Ill_{90}Chl_5C/S_5$	270±30
Bursa area	SW	7249	N40°04'43.240" E29°00'22.452"	Nilüfer Unit	phyllites							340±30
		7370	N40°05'50.376" E28°56'28.779"	Nilüfer Unit	marble							340±30
		7369	N40°10'34.850" E28°58'26.259"	Nilüfer Unit	marble							405±24
		IF 36	N40°04'25.935" E28°59'53.575"	Orhanlar Unit	dark grey mudstone with slaty cleavage	3.177±0.13 (36)	0.23	0.26		$Ms_{30}Chl_{20}Qtz_{15}Pl_{30}Cal_5$	$Ill_{60}Chl_{40}$	
		IF 37	N40°04'25.935" E28°59'53.575"	Orhanlar Unit	dark grey mudstone with slaty cleavage		0.26	0.26		$Ms_{20}Chl_{25}Qtz_{20}Pl_{35}$	$Ill_{50}Chl_{50}$	340±30
		IF 39	N40°04'23.375" E28°59'08.330"	Orhanlar Unit	grey mudstone	1.747±0.09 (46)	0.52	0.44	95	$Ms_{15}Chl_{15}Qtz_{35}Pl_{35}$	$Ill_{65}Chl_{35}$	
	NE	IF 7	N40°15'34.206" E29°13'01.968"	Hodul Unit	grey mudstone	1.176±0.08 (51)	0.92		85	$Ms_{25}Qtz_{65}Pl_{20}$	$Ill_{90}I/S_1$	

Note: %Ro -vitrinite reflectance; KI -Kübler Index; ÁI -Árkai Index; %I in I/S -illite content in illite-smectite; RSCM -raman spectroscopy on carbonaceous material; Ms -muscovite; Chl -chlorite; Qtz -quartz; K-feldspar; Pl -plagioclase; Cal -calcite; Kln -kaolinite Ill -illite; I/S -illite/smectite; C/S -chlorite/smectite.

Table 2. Raman spectroscopy data with palaeo-temperatures higher than 350° C.

Sample	Coordinates	Tectonostratigraphic Unit	Lithology	R2	SD	T(°C)	n	SE
7369	N40°10'34.850" E28°58'26.259"	Nilüfer Unit	marble	0,51	0,06	405	13	7
TU 224	N40°02'35.546" E29°43'03.227"	Hodul Unit	pelites	0,60	0,02	376	10	3
TU 226	N39°51'26.062" E30°37'58.748"	Nilüfer Unit	marble	0,32	0,03	497	12	4
TU 229	N39°47'05.589" E32°42'41.332"	Orhanlar Unit	slate	0,60	0,04	372	13	5
TU 242	N40°31'58.344" E35°45'20.904"	Nilüfer Unit	phyllite	0,59	0,02	380	11	3
TU 243	N40°29'36.406" E35°47'25.146"	Nilüfer Unit	phyllite	0,41	0,03	459	10	5

R2 is R2 ratio (D1 / (G+D1+D2)), SD is standard deviation for R2, T(°C) is temperature, n is number of spectra, and SE is standard error. Temperatures are calculated using the equation of Beyssac *et al.*(2002): T(°C) = -445R2 + 641.

1995). Mineralogical parameters were determined via processing of the XRD patterns by the WINFIT program (Krumm 1996) using an asymmetrical Pearson VII function (Stern *et al.* 1991; Warr & Rice 1994). The semiquantitative modal composition of the clay fraction was calculated using the method by Biscaye (1965), slightly modified to take into account the occurrence of mixed layer illite-smectite (I-S) and chlorite-smectite (C-S).

The very low-grade metamorphism was estimated on air-dried samples by using the illite Kübler Index (KI), obtained by measuring the full-width-at-half-maximum-height (Δ°**2**θ) on the (001) illite diffraction peak at about 10 Å on air-dried specimens (Kübler 1967; Guggenheim *et al.* 2002). KI data were calibrated against the CIS scale (Warr & Rice 1994) using the following regression equation: $KI_{(CIS)}$= 1.09 $KI_{(Bologna)}$ + 0.02 (R^2= 0.96) (Dellisanti *et al.* 2008). Chlorite crystallinity was evaluated using the Árkai Index (AI) (Árkai 1991) obtained measuring the full-width-at-half-maximum-height (Δ°**2**θ) on the (002) chlorite diffraction peak at about 7 Å on air-dried specimens (Árkai 1991; Guggenheim *et al.* 2002). AI data were calibrated using the equation: $AI_{(CIS)}$= 1.13 $AI_{(Bologna)}$ - 0.02 (R^2= 0.84) (Dellisanti *et al.* 2008). The occurrence of mixed layers I-S and C-S was determined on glycolated specimens applying the NEWMOD computer modelling (Reynolds 1985; Moore & Reynolds 1997).

Vitrinite Reflectance (Ro%)

Whole-rock samples were mounted on epoxy resin and polished according to standard procedures described in Bustin *et al.* (1990). Random reflectance (Ro%) was measured under oil immersion, with a Zeiss Axioplan microscope in reflected monochromatic non-polarized light. For each sample, an average of 20 measurements were taken on vitrinite fragments >5 μm and only slightly fractured. Mean reflectance and standard deviation values were then calculated.

Raman Spectroscopy on Carbonaceous Material (RSCM)

RSCM thermometry is based on the quantitative study of the degree of graphitization of carbonaceous material (CM), which is a reliable indicator of metamorphic *T*. Because of the irreversible character of graphitization, CM structure is not sensitive to the retrograde path during exhumation of rocks and depends on the maximum *T* reached during metamorphism (Beyssac *et al.* 2002). *T* can be determined in the range 330–650° C with a precision of ±50 °C due to uncertainties on petrological data used for the calibration. Relative uncertainties on *T* are, however, much smaller, probably around 10–15° C (Beyssac *et al.* 2004).

Raman spectra were obtained using a Renishaw InVIA Reflex microspectrometer (ENS Paris). We

used a 514 nm Spectra Physics argon laser in circular polarization. The laser was focused on the sample by a DMLM Leica microscope with a 100 × objective (NA= 0.90), and the laser power at the sample surface was set around 1 mW. The Rayleigh diffusion was eliminated by edge filters, and to achieve nearly confocal configuration the entrance slit was closed down to 10–15 μm. The signal was finally dispersed using a 1800 gr/mm grating and analyzed by a Peltier cooled RENCAM CCD detector. Before each session, the spectrometer was calibrated with a silicon standard. Because Raman spectroscopy of CM can be affected by several analytical mismatches, we followed closely the analytical and fitting procedures described by Beyssac *et al.* (2002, 2003). Measurements were done on polished thin sections cut perpendicular to the main fabrics (S0, S1) and CM was systematically analyzed below a transparent adjacent mineral, generally quartz. 10–15 spectra were recorded for each sample in the extended scanning mode (1000–2000 cm-1) with acquisition times from 30 to 60 s. Spectra were then processed using the software Peakfit (Beyssac *et al.* 2003).

Lahfid (2008) investigated the applicability of RSCM thermometry at lower temperatures, based on a qualitative comparison with reference spectra from the Glarus Alps of Switzerland. Although elaboration of the definitive version of the quantitative calibration is still in progress, we used a qualitative comparison with the reference spectra to determine temperature values in low-grade rocks.

Results

Clay Mineralogy

Mineralogical data of the clay fraction are reported in Table 1 and Figure 3. The <2 μm fraction is dominated by illite and chlorite, with subordinate mixed layer illite-smectite (I-S) and chlorite-smectite (C-S) recognized only in a few samples. Overall, the Hodul Unit is characterized by the predominance of illite over chlorite, whereas the Orhanlar Unit has similar percentages of illite and chlorite. The LKC (Nilüfer Unit) has a mineralogical composition similar to the Orhanlar Unit with a slight enrichment in illite content.

The illite Kübler index (KI) was used to evaluate the metamorphic grade. KI values of 0.42 and 0.25 (Δ°2θ) are established as lower and higher boundaries of the anchizone (Merriman & Frey 1999; Merriman 2005; Kübler 1967), whereas the value of 0.30 (Δ°2θ) is defined as the boundary between lower and upper anchizone. The Árkai index is correlated with the Kübler index and the values of 0.33 and 0.26 are established as boundaries between deep diagenetic zone, anchizone and anchizone-epizone, respectively (Árkai 1991).

KI values in analyzed samples range between 0.95 and 0.19, i.e. from deep diagenesis to epizone (Merriman & Frey 1999). In the Biga Peninsula KI data from the pelitic layers of the Hodul Unit range from 0.95 to 0.86 (Δ°2θ) indicating deep diagenetic conditions (samples IF24 and IF–19 in Table 1 and Figure 3). These data agree with the presence of highly ordered mixed-layer illite-smectite (I-S) with illite content of about 80% and 90% respectively (Table 1) due to an incomplete illitization reaction. In the Bandırma area KI values from the Hodul Unit range narrowly between 0.26 and 0.19, indicating high anchizone/epizone conditions.

Samples from the Bursa area belong to the Hodul Unit to the NE and to the Orhanlar Unit SW of the city (Table 1). The Hodul Unit experienced deep diagenetic conditions (sample IF7; KI= 0.92; 85% illite in I-S) whereas the Orhanlar Unit yielded contrasting results, ranging from deep diagenetic conditions (sample IF 39; KI= 0.52; 95% illite in I-S) to high anchizone-epizone (IF36 and IF37; KI= 0.23 and 0.26, respectively). In the İnegöl area about 60 km SE of Bursa sample TU224 from a pelitic horizon of the Hodul Unit yielded a KI value of 0.31, at the boundary between the low and high anchizone (Table 1).

Southwest of Ankara high anchizone conditions prevail in the Orhanlar Unit (TU 229 and TU231; KI= 0.27 and 0.26) whereas east of Ankara the same unit suffered only deep diagenetic conditions (TU233 and TU235; KI= 0.50) (Figure 3). For both the Bursa and the Ankara regions, there is general agreement between KI values and Árkai Index (AI) values from samples of the Orhanlar Unit (Table 1).

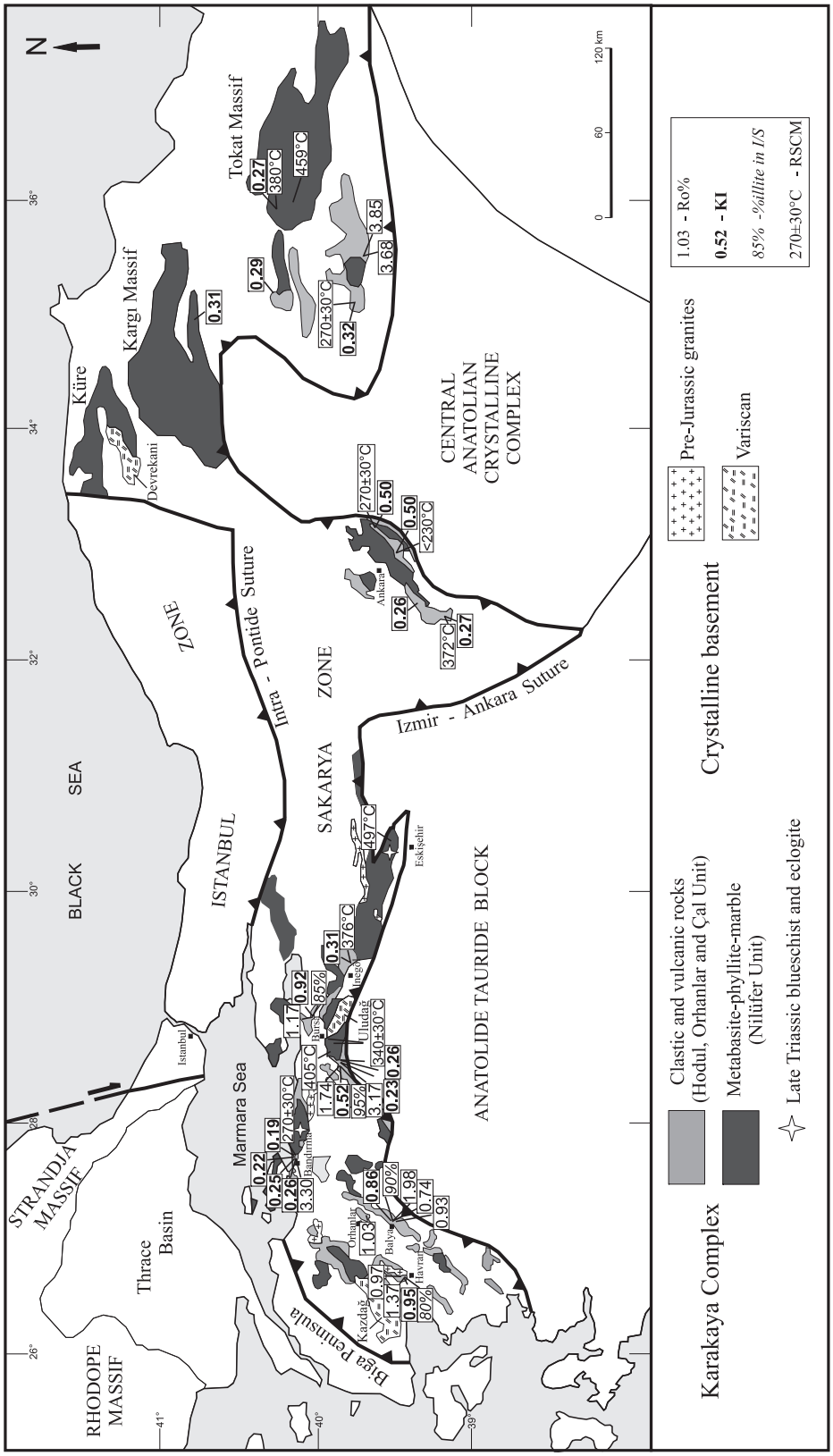

Figure 3. Geologic map of the western-central Pontides with Kübler Index and vitrinite reflectance data, and Raman spectroscopy temperatures from the Karakaya Complex. Modified from Okay & Gönciüoğlu (2004).

In the Tokat Massif KI values from the Orhanlar Unit and the LKC range from 0.32 to 0.27 (TU–237, TU–241, TU–242) indicating the boundary between low and high anchizone for both units. KI data agree with Árkai Index (AI) data (Table 1).

In the Kargı Massif one sample (TU244) was collected from the LKC. The KI value of 0.31 indicates the boundary between low and high anchizone. Again KI and Árkai Index (AI) are in agreement.

Vitrinite Reflectance (Ro%)

Kerogene is generally abundant, heterogeneous, and mainly made of poorly preserved macerals. When recognizable, macerals mainly belong to the vitrinite and inertinite groups. Where vitrinite is present, the lower Ro% measurements are representative of indigenous woody fragments and are characterized by a gaussian distribution, whereas the higher Ro% values show a less regular distribution and are mostly made up of altered or recycled fragments. Pyrite, either finely dispersed or in small globular aggregates, is generally present around vitrinite grains. Overall, Ro% mean values cover a wide range between 0.74 and 3.85%, i.e. from the mid-mature stage of hydrocarbon generation in the deep diagenetic zone to high (i.e. deep) anchizone.

In more detail, in the Biga peninsula (Figure 3) Ro% data from the arkosic sandstones of the Hodul Unit (IF23, IF17, IF20) cluster between 0.74 and 0.97% (Table 1), indicating the top of the deep diagenetic zone. Pelites from the same unit (IF24, IF19) yielded higher Ro% values of 1.37 and 1.98. Ro% frequency distribution of sample IF–24 is strongly unimodal and indicates a probably indigenous population of vitrinite fragments; conversely the frequency distribution of sample IF19 is rather scattered and indicates considerable reworking. In summary, the Hodul Unit experienced a thermal evolution from middle to very mature stages of hydrocarbon generation (oil and wet gas) in deep diagenetic conditions. The only sample taken from the Orhanlar Unit in the Biga Peninsula (IF13) yielded an Ro% value of 1.03, in general agreement with the samples from the Hodul Unit in the same area.

In the Bandırma area reliable Ro% data were obtained only from sample IF33 (Hodul Unit) with values indicating anchizone conditions (Ro%= 3.3).

Northeast of Bursa sample IF7 from Hodul Unit pelites is characterized by abundant reworked material; nevertheless the Ro% value of the possible indigenous population is 1.17%, indicating the deep diagenetic zone. Southwest of Bursa two samples from Orhanlar Unit greywackes were analyzed (Table 1). IF39 has a mean Ro% of about 1.7% in the deep diagenetic zone for a possible indigenous population, but with abundant reworked vitrinite fragments. IF–36 yielded much higher values (mean Ro of about 3.1%) correlatable with the middle anchizone.

In the Tokat area, Ro% data from Orhanlar Unit greywackes range between 3.6% and 3.8%, indicating high anchizone conditions.

Raman Spectroscopy on Carbonaceous Material (RSCM)

Raman spectroscopy-derived temperatures of analyzed samples range between 270° C and 497° C. Samples which yielded temperatures <350° C and >350° C are listed in Tables 1 and 2, respectively. Representative Raman spectra and corresponding RSCM temperatures for samples with temperatures >350° C are shown in Figure 4.

Samples from the Hodul Unit in the Bandırma area (IF28, IF29, IF31, IF33, IF34) (Figure 3) recorded temperatures <300° C. As mentioned above, in this case temperature estimates are based on a semiquantitative approach and the result is a homogeneous value of 270±30° C for all samples, suggesting that in this area the Hodul Unit underwent very low-grade metamorphic conditions.

In the Bursa area, samples 7249, 7370, 7369 were taken from the LKC phyllite and marble. Sample 7369 yielded a temperature of 405° C whereas for samples 7249 and 7370 temperature estimates reach 340±30° C.

In the area south of İnegöl and north of Eskişehir, peak metamorphic temperatures are 376°C (TU224 from the Hodul Unit) and 497°C (TU226 from a marble layer of the LKC) respectively.

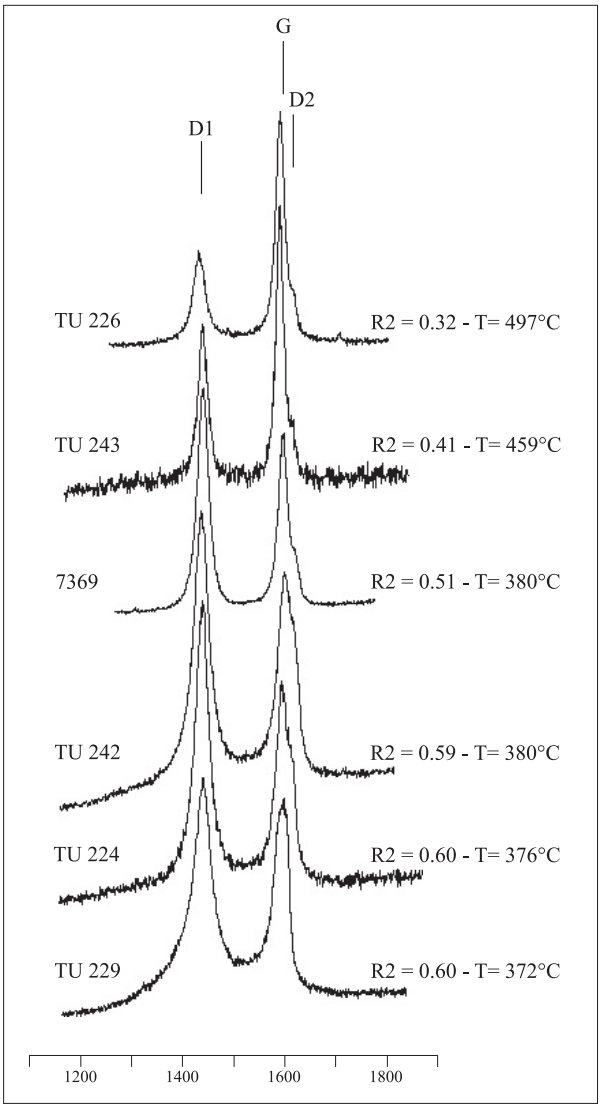

Figure 4. Raman spectra of carbonaceous material obtained in various units of the Karakaya Complex in order of increasing metamorphic grade. Locations are indicated in Figure 3. Position of the graphite G band and D1, D2 defects bands are indicated. For each spectrum, the value of the mean R2 ratio (R2= D1/[G+D1+D2] peak area ratio) obtained after 10 decompositions and corresponding RSCM temperature is given.

RSCM data from the Orhanlar Unit in the Ankara area show an increase in temperatures from northeast (TU233 and TU235; <230° C and 270±30° C, respectively) to southwest (TU229; 372° C).

In the Tokat Massif two samples were collected. South of the massif, sample TU237 from the Orhanlar Unit yielded a temperature of 270±30° C; in the northern part of the massif sample TU243 from the LKC yielded a temperature of 459° C.

Discussion

The results of this research, integrated with pre-existing petrological data (Genç & Yılmaz 1995; Okay & Monié 1997; Yılmaz *et al.* 1997; Yılmaz & Yılmaz 2004; Okay et al. 2002, 2006), provide a comprehensive thermal characterization of the Karakaya Complex of northern Anatolia. In Figure 5 the palaeotemperatures obtained from clay mineralogy, vitrinite reflectance, and Raman microspectroscopy are summarized. Overall, two main thermal conditions could be recognized: a deep diagenetic condition in the Biga Peninsula to the west and a much higher thermal condition, from low anchizone to epizone, to the east. Some samples taken southwest of Bursa and northeast of Ankara, however, seem to contradict this general pattern.

Okay and others (1991, figure 13) depict the Orhanlar Unit in the Biga Peninsula as regionally thrust over the Hodul Unit. A later (probably late Tertiary) near-vertical fault brought down the Orhanlar Unit and juxtaposed it to the Hodul Unit. We found no substantial difference between hanging wall and footwall thermal maturity, indicating that their thermal signature was acquired in an almost homogeneous shallow environment (deep diagenetic environment; 4–5 km of depth) in a range of 125–140° C, probably after both thrusting and later high-angle faulting. The lack of a well-developed cleavage in the mudstones indicates negligible illite recrystallization during diagenetic processes, confirming low burial depths and temperatures. Apatite fission-track data acquired on the same units (Cavazza *et al.* 2009) indicate temperatures higher than 125° C (total resetting).

In the Bandırma area (Figure 3), Ro, KI, and RSCM data from the Hodul Unit indicate anchizone-epizone conditions, suggesting that the thermal signature was acquired in a much deeper environment (8–9 km) than the same unit in the Biga Peninsula (Figure 5). In this locality, the Hodul Unit tectonically overlies the LKC (Nilüfer Unit). Okay & Monié (1997) described the LKC in this area as a >5

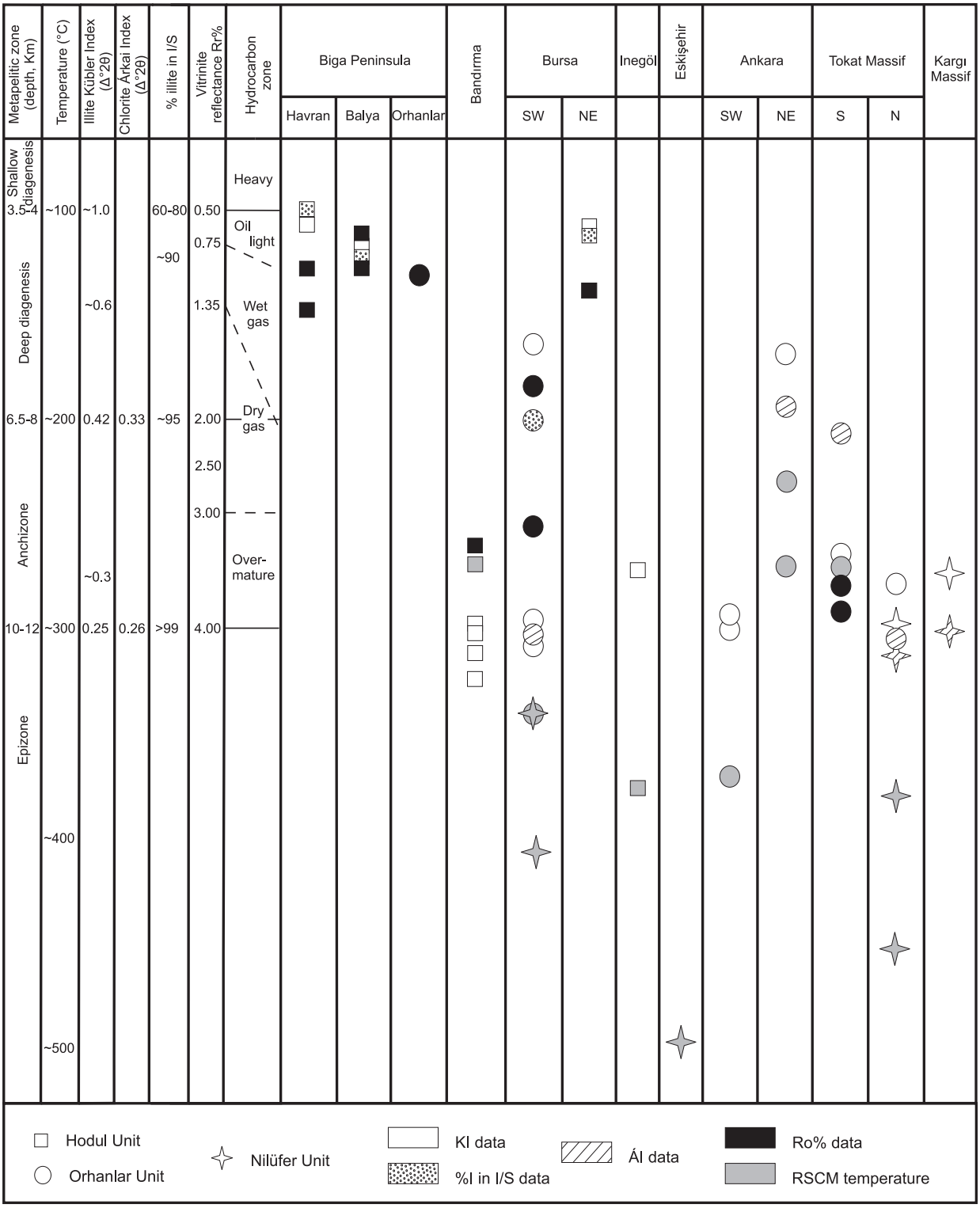

Figure 5. Regional distribution of clay mineral, vitrinite reflectance and Raman spectroscopy data. For ÁI only values between 0.33 and 0.26 are reported. For RSCM the mean temperatures are indicated.

km thick succession, mainly comprising greenschist facies metabasite containing actinolite or barroisite + albite + epidote + chlorite + titanite. Within the metabasite, a tectonic lens of eclogite occurs with a mineral paragenesis indicating high pressure-low temperature metamorphism, whereas the enclosing metabasite shows no evidence of high pressure metamorphism. Geochronological data ($^{40}Ar/^{39}Ar$) from the eclogite gave an age for the metamorphic peak between 208 and 203 Ma (Triassic–Jurassic boundary) (Okay & Monié 1997). The radiometric age is consistent with stratigraphic data, as lower Jurassic deposits unconformably overlie the metamorphic rocks.

Northeast of Bursa, Ro and clay mineralogy data from the Hodul Unit (Figures 3 & 5) indicate deep diagenetic conditions, suggesting a thermal path with no substantial differences from that in the same unit on the Biga peninsula. Southwest of Bursa the LKC is characterized by high-pressure greenschist facies metamorphism with a mineral assemblage of actinolite/barroisite + epidote + chlorite + albite + leucoxene; within the green metabasite there is an epidote blueschist band with a mineral assemblage of quartz + sodic amphibole + epidote + albite (Okay 2004). As there is no evidence for polymetamorphism in these rocks, it could be the result of cogenetic metamorphism in the P-T region of transition between blueschist and greenschist facies (Okay 2004). Kisch *et al.* (2006) provided mean b_0 data of 9.039 Å from the same unit and suggested it was subjected to intermediate to high pressure metamorphism in a convergent basin setting with a low geothermal gradient (Merriman 2005). RSCM and b_0 data agree with petrological data described by Okay (2004) indicating low-grade metamorphic conditions for the LKC in this area. Our data provide further constraints as RSCM temperatures from the phyllite and marble of the LKC range between 340±30° C and 405° C (Table 1).

In the same area the Orhanlar Unit shows peak temperatures from deep diagenesis to high anchizone/epizone (Figure 5), corresponding to a burial depth from 5–6 to 9–10 km. The progressive change in thermal conditions is confirmed by a different development of microfabric and bulk mineralogy of mudstone samples (Kisch 1987; Merriman & Frey 1999). Mudstones in diagenetic conditions show a bedding-parallel fabric, whereas high anchizone and epizone conditions feature slaty cleavage and increased illite-muscovite/quartz ratios due to recrystallization of strongly oriented illite and muscovite (Norris & Rupke 1986). These estimates agree with temperatures obtained by RSCM (340±30° C).

Further east, KI data from the Hodul Unit in the İnegöl area (Figure 3) indicate the high/low anchizone boundary. A temperature obtained by RSCM (376° C) recorded a slightly higher thermal condition but is compatible with the KI value. In this area, the arkosic sandstone of the Hodul Unit is thrust over the LKC (Genç & Yılmaz 1995). A wedge shaped tectonic slice of meta-ophiolite, consisting of metamorphosed serpentinite, gabbro and basalt, is also present in this area (Genç & Yılmaz 1995).

North of Eskişehir, eclogite and blueschist facies rocks occur as a thrust sheet within the greenschist facies of the LKC. The common blueschist facies mineral assemblage in the metabasite is sodic-amphibole + epidote + albite + chlorite + phengite ± garnet. An eclogite paragenesis of garnet + sodic pyroxene + sodic-calcic amphibole + epidote was found only in one locality (Okay *et al.* 2002). P-T conditions of the epidote-blueschist facies metamorphism have been estimated as 450±50° C and 11-12 kbar, whereas the very low Na contents of calcic amphiboles in the greenschist facies metabasites indicate pressure <4 kbar (Okay *et al.* 2002). RSCM data (497° C) from a marble layer of the metabasite of the LKC agree with the petrological data. Again, phengite, sodic amphibole and barroisite $^{40}Ar/^{39}Ar$ ages from the metabasite range between 215–205 Ma and indicate Late Triassic high pressure metamorphism, similar to that found in the Bandırma eclogite (Okay *et al.* 2002).

In the Ankara region, samples from the Orhanlar Unit record two somewhat different thermal evolutions (Figures 3 & 5). KI and RSCM data from samples TU–229 and TU–231 indicate palaeotemperatures typical of the high anchizone and the top of the epizone. However, KI data from samples TU233 and TU235 indicate only deep diagenetic conditions. The different thermal paths observed in the Ankara region could derive from

tectonic deformation. In fact, samples indicating high anchizone and epizone conditions show a closely spaced slaty cleavage due to recrystallization and orientation of platy minerals, mostly illite-muscovite, as a consequence of progressive burial at temperatures of about 200–300° C. In contrast, samples with higher KI values show a spaced slaty cleavage typical of tectonic shear. Shear strain can induce lattice defects in the illite structure leading to estimates of higher KI values (Árkai *et al.* 2002; Abad *et al.* 2003) and consequently to apparent lower thermal conditions. Thus, the samples could have had the same thermal history but different subsequent tectonic evolution, as also shown by the higher RSCM temperatures obtained from the tectonically deformed samples.

In the Tokat Massif, the LKC was affected by regional greenschist facies metamorphism as the mineral paragenesis suggests pressures of 3 to 6 kbar and temperatures of 300–500° C (Rojay & Göncüoğlu 1997; Yılmaz *et al.* 1997; Yılmaz & Yılmaz 2004). Our RSCM palaeotemperature determinations (380–459° C) from the LKC fit well with the pre-existing thermobarometric reconstructions (Figures 3 & 5). KI, Ro, and RSCM palaeotemperature determinations from the Orhanlar Unit indicate homogeneous thermal conditions at about 270–300° C.

In the Kargı Massif, our results on the LKC (Figures 3 & 5) agree with the high pressure greenschist facies regional metamorphism suggested by Okay *et al.* (2006).

In summary, moving from west to east (Figure 5) the Hodul Unit recorded peak thermal conditions from diagenesis (Biga Peninsula) to anchizone and epizone (Bandırma and İnegöl). This increase in thermal conditions is interrupted northeast of Bursa, where the Hodul Unit records only deep diagenetic conditions. Similar geographic trends were recorded by the Orhanlar Unit. In fact, data from organic and inorganic parameters for this unit range from deep diagenetic condition in the Biga Peninsula to anchizone and epizone around Bursa, Ankara, and in the Tokat Massif. This coherent geographic trend is somehow interrupted in the Ankara region, where deep diagenetic and low anchizone conditions were recorded. Data from the LKC are fully concordant with those pre-existing thermobarometric reconstructions and peak temperatures determined during this study are everywhere higher than those from the Upper Karakaya Complex. KI data indicate high anchizone conditions and RSCM temperatures (ranging between 340±30° C to 497° C) along with petrological data indicate greenschist facies metamorphism. The highest peak temperature metamorphism detected here is from Bursa, Eskişehir and in the Tokat Massif areas.

The integrated dataset (clay mineralogy, vitrinite reflectance, Raman microspectroscopy) obtained during this study is in agreement with clay mineralogy data recently obtained from the Karakaya Complex by Tetiker et al. (2009a, b). For example, Tetiker et al. (2009b, Figure 12) report KI values from the UKC in the area between Edremit and Bursa ranging from 0.85 and 0.30. Our average KI value from the same region is 0.62 ± 0.33, if we exclude the results obtained from samples taken around Bandırma, an area not sampled by Tetiker at al. (2009b). Similarly, KI values obtained by Tetiker at al. (2009b, Figure 6) from the Tokat Massif cluster at 0.15-0.30 for the LKC and 0.25-0.40 for the UKC, again in agreement with our data (Table 1). Reconstructed peak thermobarometric conditions (Tetiker et al. 2009a, Figure 8; 2009b, Figure 17) of 14 Kb/500 °C for the LKC and 5 Kb/300° C for the UKC are in agreement with our temperature reconstructions constrained by multiple methods.

The results of this study and the preexisting data available in the literature are still insufficient to fully discriminate among the various hypotheses put forward to explain the development of the Karakaya Complex. For the LKC a wealth of data on textural features, mineral associations, clay/phyllosilicate transformations, typical index minerals, and crystallochemistry of various mineral species points to HP/LT conditions in a compressional basin (Okay & Moniè 1997; Rojay & Göncüoğlu 1997; Okay et al. 2002; Tetiker et al. 2009a, b). More difficult is the interpretation of the UKC for which a rather limited dataset is available. According to Tetiker et al. (2009b), the Upper Karakaya units (Orhanlar, Hodul, Çal, and their eastern equivalents) reflect the diagenetic/metamorphic characteristics of an extensional basin dominated by low heat flow. We do

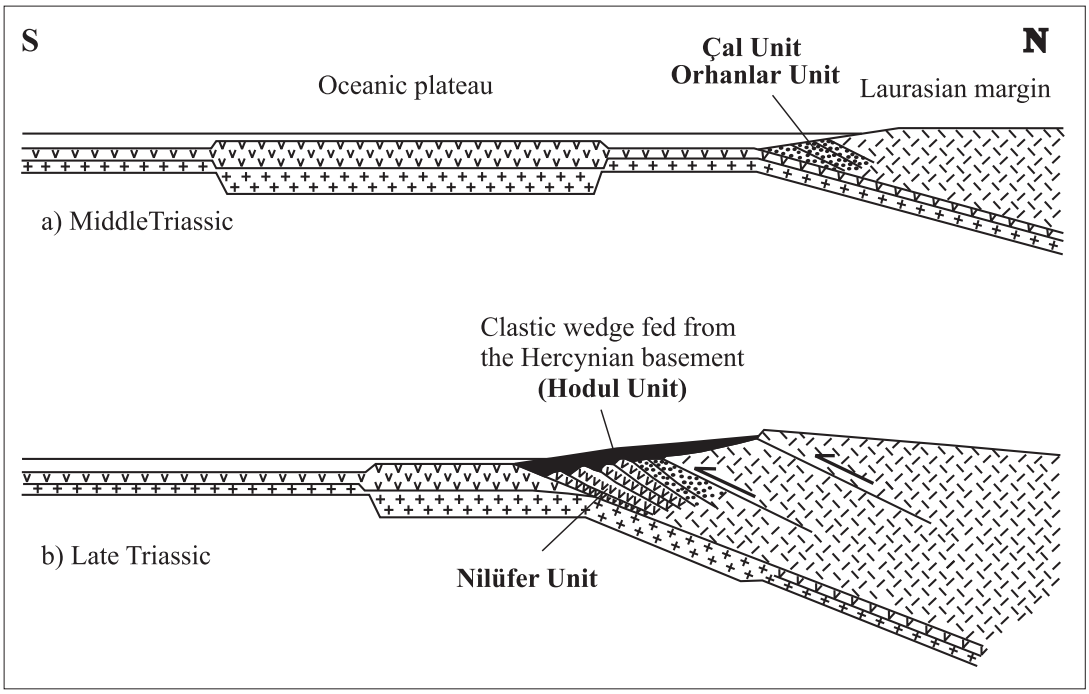

Figure 6. Schematic cross-section showing the hypothetical tectonic evolution of the Karakaya Complex during the **(a)** Middle Triassic and **(b)** Late Triassic. Modified from Okay (2000).

not share their opinion, as low heat flow is a hallmark of sedimentary basins located along subduction zones and partly or totally superposed on subduction-accretion complexes such as forearc, trench-slope, or peripheral foreland basins (e.g. Ingersoll & Busby-Spera 1995; Allen & Allen 2005).

The thermal evolution of the Karakaya Complex may be envisaged as the result of Permo–Triassic subduction-accretion related to the progressive closure of the Palaeotethys Ocean (Figure 6). Within the framework of the oceanic-plateau hypothesis of Okay (2000), during the Middle Triassic, while the Lower Karakaya (Nilüfer Unit) oceanic plateau was moving towards the southern active margin of Laurasia, the greywacke series of the Upper Karakaya (Orhanlar Unit) were probably already part of the accretionary complex. In the Late Triassic, the LKC was accreted, as testified by the presence of the eclogite and blueschist facies slices. During this stage, deformation along the Laurasian margin induced erosion of granitic basement and sedimentation of arkosic detritus (Hodul Unit) onto the accretionary wedge. The different temperature peaks (120–376° C) recorded in the Upper Karakaya are the results of different degree of involvement of the units in the complex dynamic processes of the accretionary wedge. Portions of these units experienced high temperatures in the deepest sections of the accretionary wedge, whereas other remained at relatively shallow depths.

At the Triassic–Jurassic boundary the Karakaya Complex suffered an erosional episode (Cimmeride orogeny), and was then regionally overlain by relatively undeformed lower Jurassic shallow-marine sandstone and limestone (Figure 2). In the Bursa region, a new AFT age from the overlying Early Jurassic sandstone (Bayırköy Formation) yielded a Middle Jurassic age (184±22 Ma), showing that such sandstone was never buried more than a few kilometres down (Okay *et al.* 2008). This result constrains the exhumation history of the Karakaya Complex, which recorded Late Triassic peak temperatures and during the Jurassic was already at relatively a shallow crustal depth, at least in the Bursa region.

Conclusions

Integrated analytical methods for the determination of organic and inorganic parameters –including clay mineralogy, vitrinite reflectance and Raman spectroscopy on carbonaceous material– were applied to the Karakaya Complex of northern Anatolia to constrain its thermal structure and evolution. Such multi-method investigation shows a good degree of correlation among the results of these methods, and demonstrates that Raman spectroscopy on carbonaceous material can be applied successfully to temperature ranges of 200–350° C, thus extending the application of this method from higher grade metamorphic contexts (Bollinger *et al.* 2004; Beyssac *et al.* 2007; Gabalda *et al.* 2009) to lower grade metamorphic conditions.

Our data from the Lower Karakaya Complex (Nilüfer Unit) indicate a range of peak temperatures up to about 500° C (upper greenschist facies), with higher temperatures reached in Bursa, Eskişehir and in the Tokat Massif areas. The Hodul and the Orhanlar Units of the Upper Karakaya Complex yielded heterogeneous temperature peaks (125–376° C) across the study area. Deep diagenetic conditions (4–5 km depth), were detected in the Biga Peninsula whereas towards the east anchizone up to epizone conditions (9–10 km) prevail. The commonly held notion that the graywackes of the Orhanlar Unit suffered higher deformation and temperature than the arkoses of the Hodul Unit is disproved by the results of this study, as the two units share a common range of peak temperatures across the study area.

The thermal evolution of the Karakaya Complex as a whole is the result of complex accretionary wedge dynamics during the progressive closure of the Palaeotethys Ocean in Permo–Triassic time. At the Triassic–Jurassic boundary the Karakaya Complex was further deformed, uplifted and eroded during the Cimmerian collisional orogeny. The Complex is overlain by a relatively undeformed Early Jurassic succession which was never buried more than a few kilometres down, suggesting that (i) most of the Karakaya Complex was already at shallow crustal depth by Early Jurassic time and hence (ii) its thermal evolution can be ascribed to subduction-accretion processes.

Acknowledgments

Two anonymous reviews provided insightful criticism and helped improving the manuscript substantially. This research was sponsored by MIUR (Italian Department of Public Education, University and Research) and by TÜBA (The Turkish Academy of Sciences). Field assistance by Selvihan Göktak is gratefully acknowledged.

References

Abad, I., Guitierrez-Alonso, G., Nieto, F., Gertner, I., Becker, A. & Cabro, A. 2003. The structure and the phyllosilicates (chemistry, crystallinity and texture) of Talas Ala-Tau (Tien Shan, Kyrgyz Republic): comparison with more recent subduction complexes. *Tectonophysics* **365**, 103–127.

Akyürek, B., Bilginer, E., Akbaş, B., Hepşen, N., Pehlivan, Ş., Sunu, O., Soysal, Y., Dağer, Z., Çatal, E., Sözeri, B., Yldirim, H. & Hakyemez Y. 1984. Basic geological features of the Ankara-Elmadağ-Kalecik region. *Jeoloji Mühendisliği* **20**, 31–46 [in Turkish with English abstract].

Akyürek, B. & Soysal, Y. 1983. Basic geological features of the region south of the Biga Peninsula (Savaştepe-Kırkağaç-Bergama-Ayvalık). Maden *Tetkik ve Arama Enstitütü (MTA) Dergisi* **95/96**, 1–13 [in Turkish with English abstract].

Aldega, L., Botti, F. & Corrado, S. 2007a. Clay mineral assemblages and vitrinite reflectance in the Laga Basin (Central Apennines, Italy): What do they record? *Clays and Clay Minerals* **55**, 504–518.

Aldega, L., Corrado, S., Grasso, M. & Maniscalco, R. 2007b. Correlation of diagenetic data from organic and inorganic studies in the Apenninic-Maghrebian fold-and-thrust belt: a case study from Eastern Sicily. *The Journal of Geology* **115**, 335–353.

Allen, P.A. & Allen, J.R. 2005. *Basin Analysis – Principles and Applications.* Blackwell Publishing.

Altiner, D. & Koçyiğit, A. 1993. Third remark on the geology of the Karakaya basin. An Anisian megablock in northern central Anatolia: micropaleontologic, stratigraphic and structural implications for the rifting stage of the Karakaya basin. *Revue de Paléobiologie* **12**, 1–17.

Árkai, P. 1991. Chlorite crystallinity: an empirical-approach and correlation with illite crystallinity, coal rank and mineral facies as exemplified by Paleozoic and Mesozoic rocks of Northeast Hungary. *Journal of Metamorphic Geology* **9**, 723–734.

Árkai, P., Ferreiro Mählmann, R., Suchy, V., Balogh, K., Sykorova, I & Frey, M. 2002. Possible effects of tectonic shear strain on phyllosilicate: a case study from the Kandersteg area, Helvetic domain, Central Alps Switzerland. *Schweizerische Mineralogische und Petrographische Mitteilungen* **82**, 273–290.

Beyssac, O., Bollinger, L., Avouac, J.P. & Goffè, B., 2004. Thermal metamorphism in the lesser Himalaya of Nepal determined from Raman spectroscopy of carbonaceous material. *Earth and Planetary Science Letters* **225**, 233–241.

Beyssac, O., Goffè, B., Chopin, C. & Rouzaud J.N. 2002. Raman spectra of carbonaceous material in metasediments: a new geothermometer. *Journal of Metamorphic Geology* **20**, 859–871.

Beyssac, O., Goffè, B., Petitet, J.P., Froigneux, E., Moreau, M. & Rouzaud J.N. 2003. on the characterization of disordered and heterogeneous carbonaceous materials by Raman spectroscopy. *Spectrochimica Acta Part A* **59**, 2267–2276.

Beyssac, O., Simoes, M., Avouac, J.P., Farley, K.A., Chen, Y.G., Chan Y.C. & Goffè, B. 2007. Late Cenozoic metamorphic evolution and exhumation of Taiwan. *Tectonics* **26**, TC6001, doi:10.1029/2006TC002064.

Bingöl, E., Akyürek, B. & Korkmazer, B. 1975. Geology of the Biga Peninsula and some characteristic of the Karakaya blocky series. *In*: *Congress of Earth Sciences on the Occasion of the 50th Anniversary of the Turkish Republic*, 70–77[in Turkish with English abstract].

Biscaye, P.E. 1965. Mineralogy and sedimentation of recent dee-sea clay in the Atlantic ocean and adiacent seas and oceans. *Geological Society of America Bullettin* **76**, 803–832.

Bollinger, L., Avouac, J.P., Beyssac, O., Catlos, E.J., Harrison, T.M., Grove, M., Goffè, B. & Sapkota, S. 2004. Thermal structure and exhumation history of the Lesser Himalaya in central Nepal. *Tectonics* **23**, TC5015, doi:10.1029/2003TC001564.

Bustin, R.M., Barnes, M.A. & Barnes, W.C. 1990. Determining levels of organic diagenesis in sediments of fossil fuels. *In*: McIlreath, I.A. & Morrow, D.W. (eds), Diagenesis, Geoscience Canada Reprint, 205–226.

Cavazza, W., Federici, I., Okay, A.I. & Zattin M. 2010. Pre-Cenozoic amalgamation of the İstanbul and Sakarya terranes (NW Turkey) – evidence from low-temperature thermochronology. *Terra Nova*, submitted.

Corrado, S., Aldega, L., Di Leo, P., Giampaolo, C., Invernizzi, C., Mazzoli, S. & Zattin, M., 2005. Thermal maturity of the axial zone of the Southern Apennines fold-and thrust-belt (Italy) from multiple organic and inorganic indicators. *Terra Nova* **17**, 56–65.

Dellisanti, F., Pini G., Tateo, F. & Baudin, F. 2008. The role of tectonic shear strain on the illitization mechanism of mixed-layers illite-smectite. A case study from a fault zone in the Northern Apennines, Italy. *International Journal of Earth Sciences* **97**, 601–616.

Ferreiro Mählmann, R. 2001. Correlation of very low grade data to calibrate a thermal maturity model in a nappe tectonic setting, a case study from the Alps. *Tectonophysics* **334**, 1–33.

Gabalda, S., Beyssac, O., Jolivet, L., Agard, P. & Chopin C. 2009. Thermal structure of fossil subduction wedge in the Western Alps. *Terra Nova* **21**, 28–34.

Genç, Ş.C. & Yilmaz, Y. 1995. Evolution of the Triassic continental margin, northwest Anatolia. *Tectonophysics* **243**, 193–207.

Göncüoğlu, M.C., Kuwahara, K., Tekin, U.K. & Turhan, N. 2004. Upper Permian (Changxingian) Radiolarian cherts within the clastic successions of the 'Karakaya Complex' in NW Anatolia. *Turkish Journal of Earth Sciences* **13**, 201–213.

Göncüoğlu, M.C., Turhan, N., Şentürk, K., Özcan, A. & Uysal, Ş. 2000. A geotraverse across NW Turkey: tectonic units of the central Sakarya region and their tectonic evolution. *In*: Bozkurt E., Winchester J.A. & Piper J.D.A. (eds) *Tectonics and Magmatism in Turkey and Surrounding Area.* Geological Society, London, Special Publications **173**, 139–161.

Guggenheim, S., Bain D.C., Bergaya, F., Brigatti, M.F., Drits, V.A., Eberl, D.D., Formoso, M.L.L., Galan, E., Merriman, R.J., Peacor, D.R., Stanjek, H. & Watanabe, T. 2002. Report of the Association Internationale pour l'Etude des Argiles (AIPEA) Nomenclature Committee for 2001: order, disorder and crystallinity in phyllosilicates and the use of the 'Crystallinity Index'. *Clay Minerals* **37**, 389–393.

Ingersoll, R.V. & Bubsy-Spera, C.J. 1995. Tectonics of Sedimentary Basins. Blackwell Science.

Judik, K., Rantitsch, G., Rainer, T.M., Árkai, P. & Tomljenović, B. 2008. Alpine metamorphism of organic matter in metasedimentary rocks from Mt. Medvednica (Croatia). *Swiss Journal of Geoscience* **101**, 605–616.

Kaya, O. & Mostler, H. 1992. A Middle–Triassic age for low-grade greenschist facies metamorphic sequence in Bergama (İzmir), western Turkey: the first paleontological age assignment and structural-stratigraphic implications. *Newsletter for Stratigraphy* **26**, 1–17.

Kaya, O., Wiedmann, J. & Kozur, H. 1986. Preliminary report on the stratigraphy, age and structure of the so-called Late Paleozoic and/or Triassic 'mélange' or 'suture zone complex' of northwestern and western Turkey. *Yerbilimleri* **13**, 1–16.

Kisch, H.J. 1987. Correlation between indicators of very low-grade metamorphism. *In*: Frey, M. (ed), *Low Temperature Metamorphism*. Blackie, Glasgow, 227–300.

Kisch, H.J. 1991. Illite crystallinity – Recommendations on sample preparation, X-ray-diffraction settings, and interlaboratory samples. *Journal of Metamorphic Geology* **9**, 665–670.

Kisch, H.J., Sassi, R. & Sassi, F.P. 2006. The b_0 lattice parameter and chemistry of phengites from HP/LT metapelites. *European Journal of Mineralogy* **18**, 207–222.

Koçyiğit, A. 1987. Tectonostratigraphy of the Hasanoğlan (Ankara) region: evolution of the Karakaya orogenic belt. *Yerbilmeri* **14**, 269–294 [in Turkish with English abstract].

Krumm, S. 1996. WINFIT 1.0 – A computer program for X-ray diffraction line profile analysis. *Acta Universitatis Carolinae Geologica* **38**, 253–261.

Kozur, H., Aydin, M., Demir, O., Yakar, H., Göncüoğlu, M.C. & Kuru, F. 2000. New stratigraphic and palaeogeographic results from Palaeozoic and Early–Mesozoic of the Middle Pontides (northern Turkey) in the Azdavay, Devrekani, Küre and İnebolu areas. Implications for the Carboniferous–Early Cretaceous geodynamic evolution and some related remarks to the Karakaya oceanic rift basin. *Geologica Croatica* **53**, 209–268.

Kübler, B. 1967. La cristallinité de l'illite et les zones tout à fait supérieures du métamorphisme. *In*: *Etages Tectoniques, Colloque de Neuchâtel 1966*. Université Neuchâtel, Switzerland, 105–121.

Lahfid, A. 2008. *Etablissement d'un géothermomètre à maxima pour les séries argileuses peu matures*. PhD Dissertation, Université Paris 7 [unpublished].

Leven, E.JA. & Okay, A.I. 1996. Foraminifera from the exotic Permo-Carboniferous limestone blocks in the Karakaya Complex, northwest Turkey. *Rivista Italiana di Paleontologia e Stratigrafia* **102**, 139–174.

Lezzerini, M., Sartori, F. & Tamponi, M. 1995. Effect of amount of material used on sedimentation slides in the control of illite crystallinity measurements. *European Journal of Mineralogy* **7**, 819–823.

Merriman, R.J. 2005. Clay minerals and sedimentary basin history. *European Journal of Mineralogy* **17**, 7–20.

Merriman, R.J. & Frey, M. 1999. Patterns of very low-grade metamorphism in metapelitic rocks. In: Frey & Robinson (eds), *Low-Grade Metamorphism*, Blackwell, 61–107.

Moore, D.M. & Reynolds, R.C. 1997. X-Ray Diffraction and the Identification and Analysis of Clay Minerals. Oxford University Press, New York, 378 pp.

Norris, R.J. & Rupke, N.A. 1986. Development of slaty cleavage in a mudstone unit from the Cantabrian Mountains, northern Spain. *Journal of Structural Geology* **8**, 871–878.

Okay, A.I. 2000. Was the Late Triassic orogeny in Turkey caused by the collision of an oceanic plateau? *In*: Bozkurt E., Winchester J.A. & Piper J.D.A. (eds), *Tectonics and Magmatism in Turkey and Surrounding Area.* Geological Society, London, Special Publications **173**, 25–41.

Okay, A.I. 2004. *Tectonics and High-pressure Metamorphism in Northwest Turkey*. 32nd International Geological Congress, Florence, Italy. Field Trip Guide Book P01.

Okay, A.I. & Altiner, D. 2004. Uppermost Triassic limestone in the Karakaya Complex: Stratigraphic and Tectonic Significance. *Turkish Journal of Earth Sciences* **13**, 187–199.

Okay, A.I. & Göncüoğlu, M.C. 2004. The Karakaya Complex: a review of data and concepts. *Turkish Journal of Earth Sciences* **13**, 77–95.

Okay, A.I. & Monié, P. 1997. Early Mesozoic subduction in the Eastern Mediterranean: evidence of Triassic eclogite in northwest Turkey. *Geology* **25**, 595–598.

Okay, A.I., Monod, O. & Monié, P. 2002. Triassic blueschists and eclogites from northwest Turkey: vestige of the Paleo-Tethyan subduction. *Lithos* **64**, 155–178.

Okay, A.I., Satir, M., Zattin, M., Cavazza,W. & Topuz, G. 2008. An Oligocene ductile strike-slip shear zone: the Uludağ Massif, northwest Turkey – implication for the westward translation of Anatolia. *Geological Society of American Bulletin* **120**, 893–911.

Okay, A.I., Siyako, M. & Burkan, K.A. 1991. Geology and tectonic evolution of the Biga Peninsula, northwest Turkey. *Bulletin of the Technical University of İstanbul* **44**, 191–256.

Okay, A.I. & Tüysüz, O. 1999. Tethyan sutures of northern Turkey. In: Durand B., Jolivet L., Horváth F. & Sèranne M. (eds), *The Mediterranean Basin: Tertiary Extension Within the Alpine Orogen*. Geological Society, London, Special Publications **156**, 475–515.

Okay, A.I., Tüysüz, O., Satir, M., Özkan-Altiner, S., Altiner, D., Sherlock S. & Eren R.H. 2006. Cretaceous and Triassic subduction-accretion, high-pressure/low-temperature metamorphism and continental growth in the Central Pontides, Turkey. *Geological Society of America Bulletin* **118**, 1247–1269.

Pickett, E.A. & Robertson, A.H.F. 1996. Formation of the Late Palaeozoic–Early Mesozoic Karakaya Complex and related ophiolites in NW Turkey by Paleotethyan subduction-accretion. *Journal of Geological Society, London* **153**, 995–1009.

Pickett, E.A. & Robertson, A.H.F. 2004. Significance of the volcanogenic Nilüfer Unit and related components of the Triassic Karakaya Complex for Tethyan subduction/accretion processes in NW Turkey. *Turkish Journal of Earth Sciences* **13**, 97–143.

Potel, S., Ferreiro Mählmann, R., Stern, W.B., Mullis, J. & Fre, M. 2006. Very low-grade metamorphic evolution of pelitic rocks under high-pressure/low-temperature condition, NW New Caledonia (SW Pacific). *Journal of Petrology* **47**, 991–1015.

Rantitsch, G., Grogger, W., Teichert, C., Ebner, F., Hofer, C., Maurer E.M., Schaffer, B & Toth, M. 2004. Conversion of carbonaceous material to graphite within the Greywacke Zone of the Eastern Alps. *International Journal of Earth Sciences* **93**, 959–973.

Rantitsch, G., Sachsenhofer, R.F., Hasenhüttl, C., Russegger, B. & Rainer, T.M. 2005. Thermal evolution of an extensional detachment as constrained by organic metamorphic data and thermal modeling: Graz Paleozoic Nappe Complex (Eastern Alps). *Tectonophysics* **411**, 57–72.

Reynolds, R. C. 1985. *NEWMOD, A Computer Program for the Calculation of Basal Diffraction Intensities of Mixed- layer Clay Minerals.* 8 Brook Rd., Hanover, New Hampshire 03755, USA.

Rojay, B. & Göncüoğlu, M.C. 1997. Tectonic setting of some pre–Jurassic low–grade metamorphics in northern Anatolia. *Yerbilimleri* **19**, 109-118.

Sayıt, K. & Göncüoğlu, M.C. 2009. Geochemistry of mafic rocks of the Karakaya complex, Turkey: evidence for plume-involvement in the Palaeotethyan extensional regime during the Middle and Late Triassic. *International Journal of Earth Sciences* **98**, 367-385.

Şengör, A.M.C. 1984. *The Cimmeride Orogenic System and the Tectonics of Eurasia.* Geological Society of America, Special Paper **195**.

Şengör, A.M.C. & Yilmaz, Y. 1981. Tethyan evolution of Turkey: a plate tectonic approach. *Tectonophysics* **75**, 181–241.

Şengör, A.M.C., Yilmaz, Y. & Sungurlu, O. 1984. Tectonics of the Mediterranean Cimmerides: nature and evolution of the western termination of Paleo-Tethys. *In*: Dixon J.E. & Robertson A.H.F. (eds), *The Geological Evolution of the Eastern Mediterranean.* Geological Society, London, Special Publications **17**, 77–112.

Stampfli, G.M. & Borel, G.D. 2004. The TRANSMED Transects in Space and Time: Constrains on the Paleotectonic Evolution of the Mediterranean Domain. *In*: Cavazza, W., Roure F., Spakman, W., Stampfli, G.M. & Ziegler, P.A. (eds), *The TRANSMED Atlas – The Mediterranean Region from Crust to Mantle.* Springer, Berlin Heidelberg, 53–80 (see also Appendix 3).

Stern, W.B., Mullis, J., Rahn, M. & Frey, M. 1991. Deconvolution of the first 'illite' basal reflection. *Schweizerische Mineralogische Und Petrographische Mitteilungen* **71**, 453–462.

Tekeli, O. 1981. Subduction complex of pre-Jurassic age, northern Anatolia, Turkey. *Geology* **9**, 68–72.

Tetiker, S., Yalçın, H. & Bozkaya, Ö. 2009a. Low grade metamorphism of the units from Karakaya Complex (Tokat region). Proceedings of 14th National Clay Symposium, 155-173 [In Turkish with English abstract].

Tetiker, S., Yalçın, H. & Bozkaya, Ö. 2009b. Diagenesis and low grade metamorphism of Karakaya Complex in the NW Anatolia. Yerbilimleri 30, 193–212 [In Turkish with English abstract].

Topuz, G., Altherr, R., Kalt, A., Satir, M., Werner O. & Schwartz W.H. 2004b. Aluminous granulites from the Pulur Complex, NE Turkey: a case of partial melting, efficient melt extraction and crystallisation. *Lithos* **72**, 183–207.

Topuz, G., Altherr, R., Satir, M. & Schwartz, W.H. 2004a. Low-grade metamorphic rocks from the Pulur Complex, NE Turkey: implication for the pre-Liassic evolution of the Eastern Pontides. *International Journal of Earth Sciences* **93**, 72–91.

Warr, L.N. & Rice, A.H.N. 1994. Interlaboratory standardization and calibration of clay mineral crystallinity and crystallite size data. *Journal of Metamorphic Geology* **12**, 141–152.

Wiedmann, J. Kozur, H. & Kaya, O. 1992. Faunas and age significance of the pre-Jurassic turbidite-olistostrome unit in the western parts of Turkey. *Newsletter for Stratigraphy* **26**, 133–144.

Yilmaz, Y. 1981. Tectonic evolution of the southern margin of the Sakarya Continent. *İstanbul Yerbimileri* **1**, 33–52.

Yilmaz, A. & Yilmaz, H. 2004. Geology and Structural Evolution of the Tokat Massif (Eastern Pontides, Turkey). *Turkish Journal of Earth Sciences* **13**, 231–246.

Yilmaz, Y., Serdar, H.S., Genç C., Yiğitbaş, E., Gürer Ö.F., Elmas, A., Yildirim, M., Bozcu, M., and Gürpinar, O., 1997. The geology and evolution of the Tokat Massif, South Central Pontides, Turkey. *International Geology Review*, **39**, 365–382.